Journal of Engineering and Applied Sciences 11 (11): 2490-2494, 2016
ISSN: 1816-949X


# Kinetic and Linear Equation of Adsorption by $TiO_2$ Nanofilm Coating in Photocatalytic Reactor

Sunun Khami, Wipawee Khamwichit and Charat Siripattana
Civil and Enviromental Engineering, Walailak University, Nakhonsithamarat, Thailand

**Abstract:** Nano $TiO_2$ was coated onto nanofilm synthesized from bacterial cellulose using electrospinning technique. This $TiO_2$ coated nanofilm was installed into photocatalytic reactor to study VOCs treatment system with circulation. The adsorption kinetics were applied in this study to analyse the mechanism of VOCs adsorption in photocatalytic batch reactor. Results from the study indicated that the adsorption mechanism was best defined by pseudo-second order model. Therefore, it can be implied that the adsorption process of toluene from air was taken primarily by particle surface diffusion model. Results from simplified diffusion modeling suggested that adsorption capacity got higher as and particle size increase.

**Key words:** Nano film, Nano $TiO_2$, Adsorption, Kinetic, Photocatalytic

## INTRODUCTION

Toluene is one of the typical Volatile Organic Compounds (VOCs) in the indoor environment which is emitted from decoration materials, paint and cementing compounds. In recent years, extensive research related to the removal of toluene has been reported (Li *et al*., 2016; Ren *et al*., 2016; Abbas *et al*., 2011; Zhang *et al*., 2015). Volatile Organic Compounds (VOCs) which are major air pollutants in indoor are harmful to both human health and the environment. Photodegradation based on nano $TiO_2$ is a promising method for VOCs reduction because of its superior photocatalytic activity, chemical stability, low cost and non toxicity (Bechec *et al*., 2015; Einaga *et al*., 2015; Boyd *et al*., 1947). Adsorption efficiency depends on particle size and surface area of catalyst (Figaro *et al*., 2009; Wang and Tade, 2007; Suwannahong *et al*., 2012). In which smaller particle size resulting in higher specific surface area. Metal oxide Nano $TiO_2$ has particularly high adsorption capacity for both heavy metals and organic pollutants, demonstrating themselves as promising adsorbents for removal of toxic contaminants from indoor air (Thompson *et al*., 2007; Escobar *et al*., 2016; Bianchi *et al*., 2014a, b; Rosseler *et al*., 2015). Up to date, several research studies indicated that nanofilms coated with $TiO_2$ was one the best catalyst to be used in VOCs treatment in indoor air (Mendoza *et al*., 2015 Jacoby *et al*., 1996; Chen *et al*., 2015; Batault *et al*., 2015; Mehrvar *et al*., 2000; Zou *et al*., 2006). This study elaborated adsorption mechanism of VOCs depletion in indoor air using kinetic analysis.

## MATERIALS AND METHODS

**Characterization of $TiO_2$:** Nanofilms (20-30 nm) with the area of 15×8 cm from bacterial cellulose were formed by electrospinning technique. Nanoparticle $TiO_2$ (rutile, 25 nm particle size, 99.7% from Sigma Aldrich) was dissolved in ethanol to obtain 1,2.5 and 5 Wt%, respectivety. Nanofilm was dipped into $TiO_2$ solution at room temperature then put in oven at 60°C for 1 h. The dipping process was repeated three times.

**Reactor photocatalytic:** The experiment was set up for study of VOCs removal using the $TiO_2$ coated nanofilm in photocatalytic reactor as show in Fig. 1. The batch stainless steel reactor with 700 $cm^3$ capacity was used in this study. UV lamp with 300-450 nm lamp having the highest irradiation peak at 365 nm was installed in the reactor. The intensity of ultraviolet light was approximately 520 $mW/cm^2$. Toluene solution (99.8%) was injected into batch reactor to be mixed with air (0.2 L $min^{-1}$) to obtain 200 ppm toluene concentration at

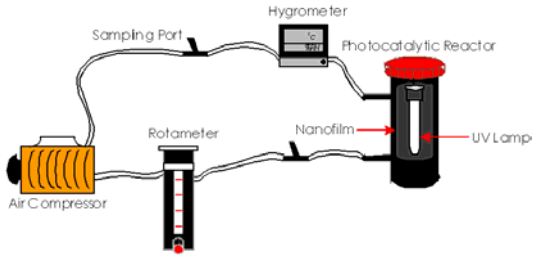


Fig. 1: Photocatalytic reactor

**Corresponding Author:** Sunun Khami, Civil and Enviromental Engineering, Walailak University Nakhonsithamarat, Thailand

steady state. Toluene contaminated air was circulated in the system for 220 mins after, toluene concentration was measured every 10 min.

## RESULTS AND DISCUSSION

**Adsorption kinetics:** Pseudo-first Order Model, Pseudo-second Order Model, Elovich Model, Intraparticle Diffusion Model and Liquid Film Diffusion Model (Boyd *et al*., 1947) were used in this study to analyse kinetic model of toluene adsorption in the photocatalytic reactor. Equation 1 expresses pseudo-first-order model in which the amount adsorbed on adsorbent at equilibrium and at time, respectively and is rate constant of pseudo-first order model:

$$\log(q_e - q_t) = \log(q_e) - \frac{k_1}{2.303}t \quad (1)$$

Pseudo-second-order model is shown in Eq. 2 in which is rate constant of pseudo-second order model:

$$\frac{t}{q_t} = \frac{1}{k_2 q_e^2} + \frac{1}{q_e}t \quad (2)$$

Equation 3 displays Elovich Model in which is initial adsorption rate and is desorption coefficient:

$$q_t = \frac{1}{\beta}\ln(\alpha\beta) + \frac{1}{\beta}\ln(t) \quad (3)$$

Intraparticle Diffusion Model is shown in Eq. 4 in which is intraparticle diffusion rate coefficient and is thickness of the boundary layer:

$$q_t = k_{int}t^{0.5} + C \quad (4)$$

Liquid film diffusion model is shown in Eq. 5 in which $K_{fd}$ is film diffusion rate:

$$-\ln\left(1 - \frac{q_t}{q_e}\right) = k_{fd}t \quad (5)$$

Figure 2 illustrates modeling results of adsorption kinetic in the photocatalytic reactor using five models as explained in the preceding section. As seen from the figure, pseudo-second order was the best model to describe toluene adsorption mechanism onto nanofilm in the reactor ($R^2 = 0.996$). The kinetic parameter used in the study was summarized in Table 1. Since, pseudo-second order model yielded the best fitting in term of $R^2$. This result suggested that adsorption process of toluene from air was dominated by particle surface diffusion model.

**Surface area and pore size by adsorption model:** Do shows that isothermal single component adsorption system with parallel pore-surface diffusion can be explained by Fickian type PDE as seen in Eq. 6:

$$\varepsilon\frac{\partial C}{\partial t} + (1-\varepsilon)\frac{\partial C}{\partial t} = \varepsilon D_p \frac{1}{r^s}\frac{\partial}{\partial r}\left(r^s\frac{\partial C}{\partial r}\right) + (1-\varepsilon)D_s\frac{1}{r^s}\frac{\partial}{\partial r}\left(r^s\frac{\partial C_\mu}{\partial r}\right) \quad (6)$$

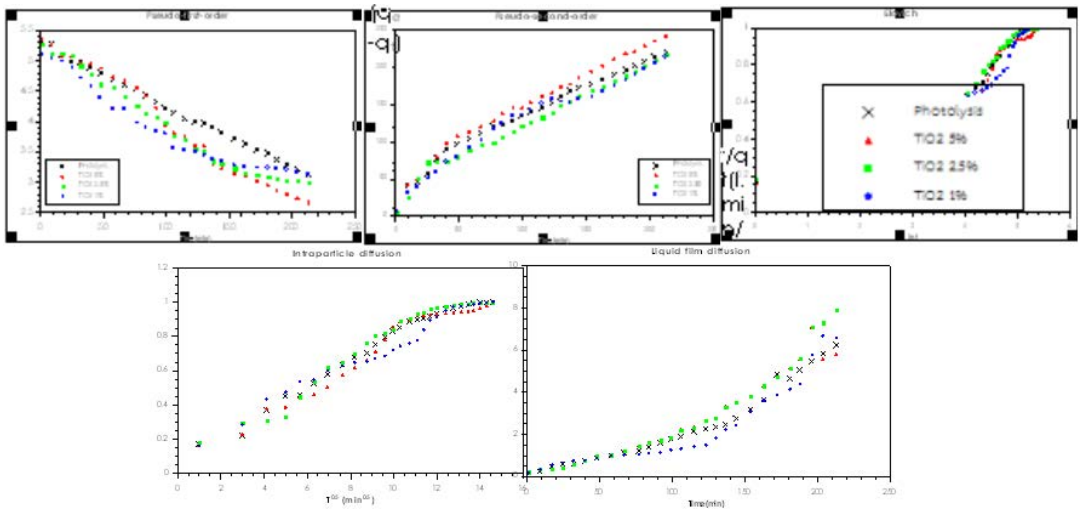


Fig. 2: Adsoption of toluene: a) Pseudo-first-order Model; b) Pseudo-second-order Model; c) Elovich Model; d) Intraparticle Diffusion Model and e) Liquid Film Diffusion Model

Table 1: Adsorption kinetics parameter of toluene by Pseudo-first-order Model, Pseudo-second-order Model, Elovich Model, Intraparticle Diffusion Model and Liquid Film Diffusion Model

| | Pseudo-first-order | | | Pseudo-second order | | Elovich | | | Intraparticle diffusion | | Liquid film diffusion | |
|---|---|---|---|---|---|---|---|---|---|---|---|---|
| Variables | $K_1$ ($min^{-1}$) | Cal.$C_t$ (mg $L^{-1}$) | $R^2$ | $K^2$ (L/mg/min) | Cal.$C_t$ (mg $L^{-1}$) | $R^2$ | α (Mg/L/min) | β (mg $L^{-1}$) | $R^2$ | $K_{int}$ (mg/L/$min^{0.5}$) | $R^2$ | $K_{fil}$ (min $L^{-1}$) |
| $TiO_2$ 1% | 0.004 | 0.691 | 0.980 | 1.166 | 0.562 | 0.995 | 0.050 | 16.181 | 0.97 | 0.062 | 0.968 | 0.027 |
| $TiO_2$ 2.5% | 0.005 | 0.716 | 0.984 | 1.151 | 0.732 | 0.997 | 0.035 | 14.663 | 0.949 | 0.068 | 0.955 | 0.034 |
| $TiO_2$ 5% | 0.006 | 0.735 | 0.981 | 1.039 | 0.896 | 0.998 | 0.017 | 14.815 | 0.954 | 0.068 | 0.924 | 0.031 |
| Photolysis | 0.004 | 0.724 | 0.981 | 1.144 | 0.986 | 0.990 | 0.035 | 14.993 | 0.974 | 0.067 | 0.957 | 0.028 |

Where:
s = Particle size factor (s = 2 for sphere)
ε = Voidage
C = Concentration

If the isotherm is assumed then linear Eq. 6 is simplified to:

$$\frac{\partial C}{\partial t} = D_{app}\nabla^2 C \quad (7)$$

where, $D_{app}$ efficiency diffusivity is defined by the following relation:

$$D_{app} = \frac{\varepsilon D_p + (1-\varepsilon)KD_s}{\varepsilon + (1-\varepsilon)K} \quad (8)$$

where, K is Henry constant which depend on temperature. For uniform initial concentration in the adsorbent, the limited fluid volume and if $\tau = \frac{D_{app}t}{R^2} > 0.2$, other terms in infinite series can be neglected and can be obtained the following approximate solution:

$$E = 1 - \left(\frac{C}{C_\infty}\right) = C\exp\left(-\frac{Sh}{2}\frac{\alpha+1}{\alpha}\right)(s+1)\frac{D_{app}t}{R^2} \quad (9)$$

When c is series coefficient or in term of adsorption rate:

$$\frac{d(1-E)}{dt} = c\left(\frac{-sh}{2}\frac{\alpha+1}{\alpha}\right)(s+1)\frac{D_{app}t}{R^2} \quad (10)$$

For $B_i = \infty$, $0.1<\alpha<\infty$ and error <10% Sherwood number was calculated using Eq. 11:

$$\frac{Sh_\infty}{2} = 3.260 - \frac{1.1067}{\gamma} + \frac{0.19179}{\gamma^2} + \frac{1.1258\times10^{-2}}{\gamma^3} \quad (11)$$

Substituting β into Eq. 9 and 12 was obtained:

$$E = 1 - c\exp(-\beta t) \quad (12)$$

The effect of varying volume ratio of fluid phase and solid phase (a) to the adsorption capacity (Eq. 9) was

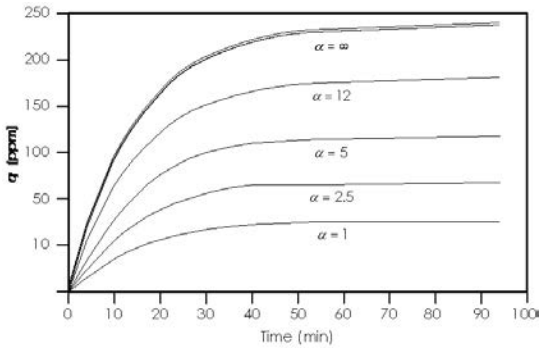


Fig. 3: Adsorption capacity at various

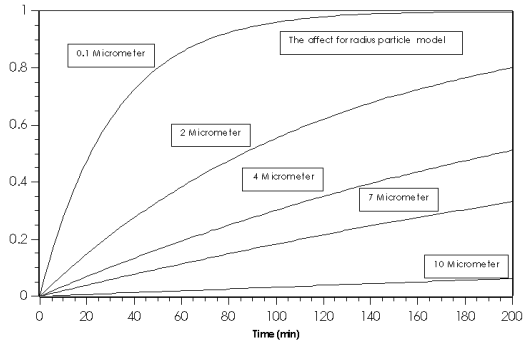


Fig. 4: The effect of particle size to the fraction adsorbed

displayed in Fig. 3. From the figure, once a got higher the adsorption capacity increases which can be explained that for the fixed volume of solid phase when increases, fluid loading is as well increased and even reaches on limiting value theoretically us a becomes infinity. This resulting in higher as increases and at gets closer to infinity equilibrium concentration in solid phase is nearly initial concentration in gas phase. Figure 4 illustrates fraction adsorbed at various particle size. Clearly seen from the figure that as particle size increases the fraction adsorbed onto catalyst surface is higher. These modeling results can be elaborated by simplified ODE of diffusion theory:

$$-\frac{d\bar{x}(t)}{dt} = K'A_e\left[\bar{x}(t) - \frac{y(t)}{m}\right]$$

## CONCLUSION

The adsorption kinetics were applied in this study to analyse the mechanism of VOCs adsorption in photocatalytic batch reactor for use in indoor air treatment. Results from the study indicated that the adsorption mechanism was best defined by pseudo-second order model. Therefore, it can be implied that the adsorption process of toluene from air was taken primarily by particle surface diffusion model. Results from simplified diffusion modeling suggested that adsorption capacity got higher as and particle size increase.

## ACKNOWLEDGEMENT

This research was financially supported by Institute of Research and Development and Research Funding Walailak University.

## REFERENCES

Abbas, N., M. Hussain, N. Russo and G. Saracco, 2011. Studies on the activity and deactivation of novel optimized TiO2 nanoparticles for the abatement of VOCs. Chem. Eng. J., 175: 330-340.

Batault, F., F. Thevenet, V. Hequet, C. Rillard, L.L. Coq and N. Locoge, 2015. Acetaldehyde and acetic acid adsorption on TiO2 under dry and humid conditions. Chem. Eng. J., 264: 197-210.

Bechec, L.M., N. Kinadjian, D. Ollis, R. Backov and S. Lacombe, 2015. Comparison of kinetics of acetone, heptane and toluene photocatalytic mineralization over TiO2 microfibers and Quartzel® mats. Appl. Catal. B. Environ., 179: 78-87.

Bianchi, C.L., E. Colombo, S. Gatto, M. Stucchi and G. Cerrato *et al*., 2014a. Photocatalytic degradation of dyes in water with micro-sized TiO2 as powder or coated on porcelain-gres tiles. J. Photochem. Photobiol. A. Chem., 280: 27-31.

Bianchi, C.L., S. Gatto, C. Pirola, A. Naldoni and D.A. Michele *et al*., 2014b. Photocatalytic degradation of acetone, acetaldehyde and toluene in gas-phase: Comparison between nano and micro-sized TiO2. Appl. Catalysis B. Environ., 146: 123-130.

Boyd, G.E., A.W. Adamson and L.S. Jr. Myers, 1947. The exchange adsorption of ions from aqueous solutions by organic zeolites II Kinetics1. J. Am. Chem. Soc., 69: 2836-2848.

Chen, K., L. Zhu and K. Yang, 2015. Tricrystalline tio 2 with enhanced photocatalytic activity and durability for removing volatile organic compounds from indoor air. J. Environ. Sci., 32: 189-195.

Einaga, H., J. Tokura, Y. Teraoka and K. Ito, 2015. Kinetic analysis of TiO 2-catalyzed heterogeneous photocatalytic oxidation of ethylene using computational fluid dynamics. Chem. Eng. J., 263: 325-335.

Escobar, S.A., M.A. Pataquiva and L.A. Vasquez, 2016. Electrocoagulation-photocatalytic process for the treatment of lithographic wastewater: Optimization using Response Surface Methodology (RSM) and kinetic study. Catal. Today, 266: 120-125.

Figaro, S., J.P. Avril, F. Brouers, A. Ouensanga and S. Gaspard, 2009. Adsorption studies of molasse's wastewaters on activated carbon: Modelling with a new fractal kinetic equation and evaluation of kinetic models. J. Hazard. Mater., 161: 649-656.

Jacoby, W.A., D.M. Blake, J.A. Penned, J.E. Boulter and L.M. Vargo *et al*., 1996. Heterogeneous photocatalysis for control of volatile organic compounds in indoor air. J. Air Waste Manage. Assoc., 46: 891-898.

Li, Y., L. Li, L. Cao and C. Yang, 2016. Promoting dynamic adsorption of Pb 2+ in a single pass flow using fibrous nano-TiO2-cellulose membranes. Chem. Eng. J., 283: 1145-1153.

Mehrvar, M., W.A. Anderson, Y.M. Moo and P.M. Reilly, 2000. Non-linear parameter estimation for a dynamic model in photocatalytic reaction engineering. Chem. Eng. Sci., 55: 4885-4891.

Mendoza, C., A. Valle, M. Castellote, A. Bahamonde and M. Faraldos, 2015. TiO2 and TiO2-SiO2 coated cement: Comparison of mechanic and photocatalytic properties. Appl. Catalysis B. Environ., 178: 155-164.

Ren, L., Y. Li, J. Hou, J. Bai and M. Mao *et al*., 2016. The pivotal effect of the interaction between reactant and anatase TiO2 nanosheets with exposed {001} facets on photocatalysis for the photocatalytic purification of VOCs. Appl. Catal. B. Environ., 181: 625-634.

Rosseler, O., U.C. Bouillet, A. Bonnefont, S. Pronkin and E. Savinova *et al*., 2015. Structural and electronic effects in bimetallic PdPt nanoparticles on TiO2 for improved photocatalytic oxidation of CO in the presence of humidity. Appl. Catalysis B. Environ., 166: 381-392.

Suwannahong, K., W. Liengcharernsit, W. Sanongraj and J. Kruenate, 2012. Application of nano-TiO2-LDPE composite film on photocatalytic oxidation degradation of dichloromethane. J. Environ. Biol., 33: 955-959.

Thompson, C.J., G.G. Chase, A.L. Yarin and D.H. Reneker, 2007. Effects of parameters on nanofiber diameter determined from electrospinning model. Polymer, 48: 6913-6922.

Wang, S., H.M. and M.O. Tade, 2007. Volatile organic compounds in indoor environment and photocatalytic oxidation: State of the art. Environ. Int., 33: 694-705.

Zhang, F., M. Wang, X. Zhu, B. Hong and W. Wang *et al*., 2015. Effect of surface modification with H2S and NH3 on TiO2 for adsorption and photocatalytic degradation of gaseous toluene. Appl. Catalysis B. Environ., 170: 215-224.

Zou, L., Y. Luo, M. Hooper and E. Hu, 2006. Removal of VOCs by photocatalysis process using adsorption enhanced TiO2-SiO2 catalyst. Chem. Eng. Process. Intensif., 45: 959-964.